

The GO4 model in near-nadir microwave scattering from the sea surface

Olivier Boisot, Frédéric Nouguier, Bertrand Chapron and Charles-Antoine Guérin

Abstract—We introduce a practical and accurate model, referred to as “GO4”, to describe near-nadir microwave scattering from the sea surface and at the same time we address the issue of the filtered mean square slope (mss) conventionally used in the Geometrical Optics model. GO4 is a simple correction of this last model taking into account the diffraction correction induced by the rough surface through what we call an effective mean square curvature (msc). We evaluate the effective msc as a function of the surface wavenumber spectrum and the radar frequency and show that GO4 reaches the same accuracy as the Physical Optics model in a wide range of incidence and frequency bands with the sole knowledge of the mss and msc parameters. The key point is that the mss entering in GO4 is not the *filtered* but the *total* slope. We provide estimation of the effective msc on the basis of classical sea spectrum models. We also evaluate the effective msc from near-nadir satellite data in various bands and show that it is consistent with model predictions. Non-Gaussian effects are discussed and shown to be incorporated in the effective msc. We give some applications of the method, namely the estimation of the total sea surface mss and the recalibration of relative radar cross-sections.

Index Terms—ocean radar sensing, near-nadir, geometrical optics, slope, curvature

I. INTRODUCTION

In spite of more than one half-century of theoretical developments in backscattering from the sea surface (e.g. [1]), the ever increasing capabilities of spaceborne microwave sensors still triggers the need for accurate, simple and versatile models for the geophysical interpretation of multi-frequency active and passive microwave data sets. Starting from the historical asymptotic theories which have a limited domain of application, many robust analytical scattering models have been developed in the last three decades [2]. Some of them have proven to

be particularly relevant for the ocean surface (e.g. [3], [4], [5], [6], [7], [8]), with a wide range of validity in terms of incidence angles, radar frequency and sea state. Now, virtually all these so-called unified models rely on the assumed knowledge of the sea surface wave number spectrum which is difficult to use in operational conditions, both from a conceptual and technical point of view. For this reason the most practical method at low incidence remains the historical Geometrical Optics (which we abbreviate to “GO2” to distinguish it from GO4) approach which relates the backscattered power to the mere probability distribution of surface slopes and is usually parametrized by the sole mean square slope (mss). However, as it is well known, this asymptotic theory is only valid in the optical limit of very short radar wavelength and can deviate significantly from the actual backscattering cross section in the microwave regime where it fails to reproduce the radar sensitivity to radar wavelength. It is often resorted to a “radar-filtered” mss ([9], [10], [11], [12], [13]) which, as we will see, is an artificial compensation of the missing diffraction term in GO2 and accounts for the fact that roughness scales much shorter than the electromagnetic (EM) wavelength are not “seen” by the radar. Even through the use of a filtered mss improves the accuracy of the GO2 model at nadir it remains very limited in incidence as corrections to the Gaussian shape of the scattering diagram must be quickly introduced. This can be partially compensated [12] by an incidence-dependent cutoff in the definition of the filtered mss but brings in an additional degree of arbitrariness. The main purpose of this paper is to propose an improved and robust version of GO2, termed GO4. The model now depends on the *total* instead of the *filtered* mss and the radar wavelength dependence is rendered through a diffraction term involving the curvature of the surface. As we will show, this makes it possible to achieve the accuracy of the Physical Optics (PO) with a very small number of parameters and makes the model very adapted to near-nadir applications where the sea surface spectrum is unknown. The GO4 model is by construction unpolarized and is therefore limited to the incidence angles where the polarization difference is negligible. It will this certainly not outperform unified

O. Boisot, F. Nouguier and C.-A. Guérin are with MIO (Mediterranean Institute of Oceanography, Université de Toulon, CNRS, Aix Marseille Université, IRD, UM 110, 83957 La Garde (olivier.boisot@univ-tln.fr, frederic.nouguier@univ-tln.fr, guerin@univ-tln.fr). O. Boisot is also with CLS/CNES, F-31400 Toulouse, France. B. Chapron is with the Laboratoire d’Océanographie Spatiale, Institut Français de Recherche pour l’Exploitation de la Mer, 29280 Plouzané, France (e-mail: bertrand.chapron@ifremer.fr).

scattering models which have been proven to be accurate over a wide range of non-grazing incidence angles and, when combined with classical sea spectra, are in satisfactory overall agreement with experimental measurements (e.g. [5], [14], [15]). The main improvement brought by GO4 is to reduce the needed characterization of the unknown sea surface, including non-Gaussian effects, to the knowledge of the mere mss and msc parameters. As a result, the arbitrariness in the choice of a “preferred” spectral model is avoided. This gain in simplicity is obtained with quasi no loss in accuracy in the domain of validity of PO.

The introduction of a curvature correction to GO2 is not new but has followed in the past different approaches and results. The overall technique is based on perturbation expansion of the scattering amplitude or the electric or magnetic surface current ([9], [10], [11], [16], [17], [18]) with respect to a well-chosen small parameter combined with higher-order Taylor expansion or cumulant expansion of the structure function of wave elevations. Some of these results and their relation to our findings will be discussed in the core of the paper. More recently, an elegant mathematical approach was proposed based on hypothesizing a generalized Student form for the slope distribution [19]. We did not pursue in this way and chose a more physical approach even though the present results have been found consistent with this last approach.

The GO4 model is introduced in Section II for isotropic Gaussian surfaces and the evaluation of the curvature parameter is given in Section III. The generalization to anisotropic and non-Gaussian sea surfaces is provided in Section IV and V, respectively. Section VI gives some applications of the GO4 model on various near-nadir data sets.

II. A SIMPLIFIED FORMALISM: THE GO4 MODEL

In the microwave regime where sea surface roughness is large, the reference model for low-angle backscattering is the Physical Optics (PO) scalar approximation. It remains accurate as long as polarization effects remain negligible, that is in the first, say, 20-25 degrees of incidence away from nadir. We recall hereafter the geometry of the scattering problem. In the following we use the notation a for the norm of any vector \mathbf{a} . We consider a rough interface $z = \eta(\mathbf{r})$ separating air (upper medium) from water (lower medium) and denote $\mathbf{r} = (x, y)$ the coordinate in the horizontal mean plane. The surface is illuminated from above by an incident monochromatic, linearly polarized, plane wave with wave vector \mathbf{K} (corresponding to wavenumber K) at some incidence angle θ with respect to the vertical direction z . In

backscattering configuration it is convenient to introduce the Ewald vector $\mathbf{Q} = -2\mathbf{K}$ together with its horizontal and vertical projections \mathbf{Q}_H and Q_z , respectively. Note that $Q_H = 2K \sin \theta$ and $Q_z = 2K \cos \theta$. The Normalized Radar Cross Section (NRCS) according to the PO approximation is expressed by the so-called Kirchhoff integral:

$$\sigma_{PO}^0 = K^2 \sec^2(\theta) |R|^2 \frac{1}{\pi} \int d\mathbf{r} e^{i\mathbf{Q}_H \cdot \mathbf{r}} e^{-\frac{1}{2}Q_z^2 S(\mathbf{r})}. \quad (\text{II.1})$$

Here R is the Fresnel coefficient at normal incidence on the surface at rest and S is the structure function of elevations:

$$S(\mathbf{r}) = 2(\rho(\mathbf{0}) - \rho(\mathbf{r})), \quad (\text{II.2})$$

which is trivially related to the roughness autocorrelation function (ρ) or, what amounts to the same, to the wave number spectrum (Ψ) through an inverse Fourier Transform:

$$\rho(\mathbf{r}) = \int d\mathbf{k} e^{i\mathbf{k} \cdot \mathbf{r}} \Psi(\mathbf{k}). \quad (\text{II.3})$$

For simplicity we assume in this section isotropicity of the wave number spectrum, so that the autocorrelation function and the PO NRCS are given by Bessel transforms:

$$\rho(r) = \int_0^\infty dk \, 2\pi k J_0(kr) \Psi(k) \quad (\text{II.4})$$

and

$$\sigma_{PO}^0 = K^2 \sec^2(\theta) |R|^2 \int d\mathbf{r} \, 2r J_0(Q_H r) e^{-\frac{1}{2}Q_z^2 S(r)} \quad (\text{II.5})$$

For large Rayleigh parameter $Q_z^2 \rho(0)$, small lags have a dominant contribution to the integral and we may approximate the structure function by its asymptotic behavior about the origin:

$$S(r) \simeq \frac{1}{2} \text{mss} \, r^2, \quad (\text{II.6})$$

where mss is the total mean square slope:

$$\text{mss} = \int_0^\infty dk \, 2\pi k \, k^2 \Gamma(k) \quad (\text{II.7})$$

Insertion of this quadratic approximation of the structure function in the Kirchhoff integral leads to the classical GO2 approximation (e.g. [1]):

$$\sigma_{GO2}^0 = \frac{|R|^2}{\text{mss}} \sec^4(\theta) \exp\left(-\frac{\tan^2 \theta}{\text{mss}}\right) \quad (\text{II.8})$$

The GO2 model is parametrized solely by the mss parameter, which is well-defined and whose wind-dependence is well characterized. It is, however, in principle only valid in the limit of small wavelengths and becomes more and more accurate as the EM frequency is increased. At finite wavelength, a curvature correction is needed to incorporate the diffraction effects and the fact that the surface deviates from its tangent plane over a few EM wavelength. To this aim we push the Taylor expansion of the structure function at the next order using a fourth-order Taylor expansion of the Bessel function in (II.4):

$$S(r) \simeq \frac{1}{2} \text{mss} r^2 - \frac{1}{32} \text{msc} r^4, \quad (\text{II.9})$$

where msc is the total mean square curvature:

$$\text{msc} = \int_0^\infty dk \, 2\pi k \, k^4 \Gamma(k) \quad (\text{II.10})$$

In defining this last quantity we assume that the fourth moment of the spectrum is finite, which implies a high-frequency cut-off on the spectrum. Again, the approximation (II.9) is asymptotically valid in the limit of small lags and can be used to define the msc:

$$\text{msc} = \lim_{r \rightarrow 0} 32 \frac{\frac{1}{2} \text{mss} r^2 - S(r)}{r^4} \quad (\text{II.11})$$

At finite lag $r > 0$ the total value of the msc is not reached but only a fraction of it, say $\beta(r)$:

$$\beta(r) \text{msc} = 32 \frac{\frac{1}{2} \text{mss} r^2 - S(r)}{r^4} \quad (\text{II.12})$$

Now the structure function in the Kirchhoff integral is only involved on a finite effective integration domain, say $[0, r_e]$ depending on the EM wavelength. On this given interval $[0, r]$, there is certainly a constant value $\text{msc}_e = \beta \text{msc}$ which optimizes in some sense the quartic approximation of the structure function:

$$S_\beta(r) \simeq \frac{1}{2} \text{mss} r^2 - \frac{1}{32} \text{msc}_e r^4 \quad (\text{II.13})$$

Note that this quartic approximation of the structure function at finite lag r does not require the finiteness of the total msc, that is the existence of a finite limit in (II.11). We chose to optimize the value of β in order to obtain the closest agreement with the PO NRCS at nadir whenever the structure function (II.2) is replaced by its quartic approximation (II.13). This amounts to equating:

$$\int_0^\infty \left(e^{-\frac{1}{2} Q_z^2 S(r)} - e^{-\frac{1}{2} Q_z^2 S_\beta(r)} \right) r dr = 0 \quad (\text{II.14})$$

Now considering S_β as a perturbation of S ,

$$S(r) = S_\beta(r) + \Delta S_\beta(r), \quad (\text{II.15})$$

with $Q_z^2 \Delta S_\beta \ll 1$, we may rewrite:

$$\int_0^\infty e^{-\frac{1}{2} Q_z^2 S(r)} (e^{\frac{1}{2} Q_z^2 \Delta S_\beta} - 1) r dr = 0 \quad (\text{II.16})$$

To evaluate this integral we use the fact that the quartic term in the exponential should be small and can be linearized, that is:

$$e^{\frac{1}{2} Q_z^2 \Delta S_\beta} \simeq e^{\frac{1}{2} Q_z^2 (S - \frac{1}{2} \text{mss} r^2)} (1 + Q_z^2 \text{msc}_e \frac{1}{64} r^4) \quad (\text{II.17})$$

This leads to the optimal msc:

$$\text{msc}_e = \frac{64 \int_0^\infty e^{-\frac{1}{2} Q_z^2 S(r)} (e^{\frac{1}{2} Q_z^2 (S - \frac{1}{2} \text{mss} r^2)} - 1) r dr}{Q_z^2 \int_0^\infty e^{-\frac{1}{4} Q_z^2 \text{mss} r^2} r^5 dr} \quad (\text{II.18})$$

To evaluate the Kirchhoff integral with the modified structure function (II.13), we again take advantage of the small magnitude of the quartic term in the exponential which can thus be linearized. This leads to the following approximation for the PO integral:

$$\begin{aligned} \sigma^0 &\simeq K^2 \sec^2(\theta) |R|^2 \frac{1}{\pi} \int d\mathbf{r} \, e^{i\mathbf{Q}_H \cdot \mathbf{r}} e^{-\text{mss} Q_z^2 \frac{r^2}{4}} \\ &\times \left(1 + \frac{1}{64} \text{msc} r^4 \right) \end{aligned} \quad (\text{II.19})$$

The evaluation of this integral can be performed routinely and leads to the following correction to the GO2 formula:

$$\begin{aligned} \sigma_{GO4}^0 &= \sigma_{GO2}^0 \times \\ &\left[1 + \frac{\text{msc}_e}{16 K^2 \text{mss}^2 \cos^2 \theta} \left(\frac{\tan^4 \theta}{\text{mss}^2} - 4 \frac{\tan^2 \theta}{\text{mss}} + 2 \right) \right], \end{aligned} \quad (\text{II.20})$$

where σ_{GO2}^0 is the GO2 NRCS with total mss.

We refer to this approximation as the ‘‘GO4’’ approximation as opposed to the GO2 model which involves only a quadratic approximation of the structure function. We call the modified curvature $\text{msc}_e = \beta \text{msc}$ the *effective mean square curvature* of the surface, which depends on the EM wavelength. This formula and the GO4 terminology were already introduced in [20] but at that time only the total and not the effective msc was considered. Note that formula (II.20) with the total curvature is equivalent to the diffraction correction developed in [18] at nadir ($X = 0$) using a iterated magnetic current integral equation.

III. THE EFFECTIVE MEAN SQUARE CURVATURE

The GO4 approximation relies on two parameters only, namely the total mean square slope mss and the effective mean square curvature msc_e . The total mss is a meaningful quantity because it quantifies the exchange surface between ocean and atmosphere or, in mathematical terms, because the decrease of the sea spectrum ensures the convergence of the second spectral moment. On the contrary, the notion of total curvature is ill-defined because it refers to the “sharpness” of wave which is ever increasing at small scales. In mathematical terms, the total msc is the fourth moment of the surface spectrum (which typically falls-off in k^{-4}) and is thus dramatically sensitive to the chosen high-frequency cut-off. This raises the issue of “where the spectrum should stop” and questions the microscopic nature of the surface. Hence, it is only the curvature at a finite scale which is meaningful. However, as it is well known, the EM scattering process performs a natural filter at the scales which cannot be “seen” by the probing EM wavelength. It is therefore clear that the total msc is not the relevant quantity to consider for the scattering process. It is more relevant to consider the effective msc of the rough surface filtered at the given EM frequency, even though the EM filtering process is somewhat more complex than a sharp cut-off on spatial frequencies. Nevertheless, we expect the effective msc to be of the order of magnitude of the fourth moment of the surface spectrum truncated at the EM wavenumber. We therefore define the dimensionless parameter α by:

$$msc_e = \int_0^{\alpha K} 2\pi k^4 \Gamma(k) dk, \quad (III.21)$$

which we expect to be close to unity. This parameter has the advantage over the alternative parameter β that it does not require the knowledge of the full msc . We have calculated the parameters α and msc_e (from II.18) for three different omnidirectional wave number spectra, referred to by the name of their first author: Elfouhaily unified spectrum [21], Bringer remote sensing spectrum [22] and Kudryavtsev physical spectrum [23], [24]. Recently, some refined short-wave spectral models have been proposed, such as a roughness spectrum based on field measurements including the effect of swell [25] or an improved directional spectrum based on stereophotography [26]. However, in the present study we will limit ourselves to the simple aforementioned omnidirectional spectra.

Figures 1 and 2 show the evolution of the parameters α and msc_e (from II.18) with the EM wavelength and wind

speed. As expected, the effective msc grows importantly with both EM frequency and wind speed and ranges over a few decades. Important relative variations (up to 20-30%) are observed between different spectral models. The cut-off parameter α , on the contrary, remains quite stable and increases only slightly with wind speed and inverse frequency. Note that $\alpha \simeq 1$ in Ka band, $\alpha \simeq 2$ in Ku band and $\alpha \simeq 2.5$ in C band.

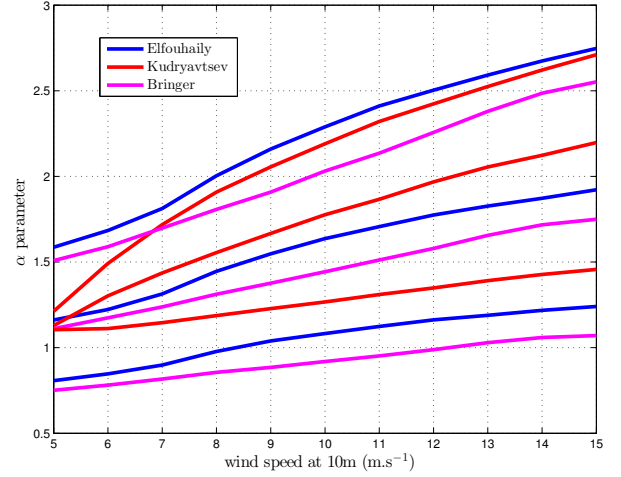


Fig. 1: Evolution of the cutoff parameter α with wind speed and EM frequency for three different models of omnidirectional spectrum: Elfouhaily (blue), Kudryavtsev (red) and Bringer (magenta). Three frequencies are shown, namely C band (upper curves), Ku band (middle curves) and Ka band (lower curves). In Ka band, the value of α is close to 1, meaning that the effective msc is approximately the total msc truncated at the EM wavelength.

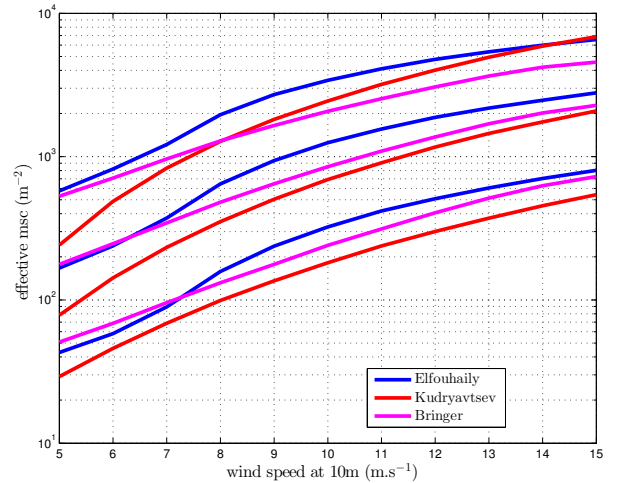


Fig. 2: Same as Figure 1 for the effective msc except that C band is lower curve and Ka band is upper curve.

Figures 3,4 and 5 show the isotropic NRCS according to GO4 with the predicted value of the cut-off parameter in the different bands: $\alpha = 1.25$ in Ka band, $\alpha = 1.89$ in Ku band and $\alpha = 2.64$ in C band. The calculation has been performed with an omnidirectional Elfouhaily

spectrum at wind speed =10 m/s. A comparison with GO2 and PO is given. The GO2 with filtered mss is also given for reference, in which the classical K/3 cut-off ([27]) is employed. Even though it brings a significant improvement over the GO2 with full mss, it is still about 1 dB away from PO at nadir. At moderate wind speed (10 m/s), an excellent agreement is found between PO and GO4 in the first 25 degrees in Ka band, the first 12 degrees in Ku band and the first 10 degrees in C band.

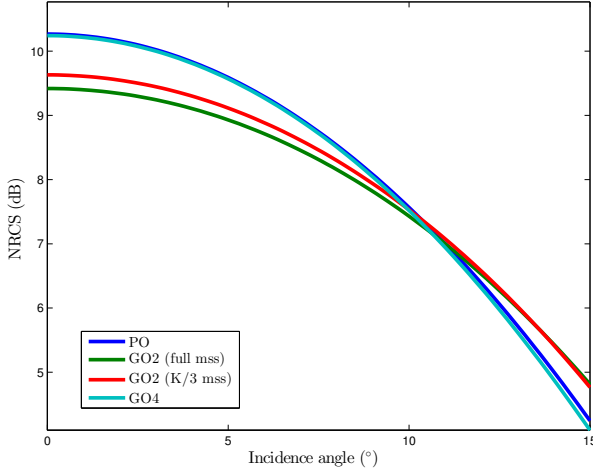


Fig. 3: Comparison of PO, GO2 and GO4 in Ka band with $\alpha = 1.26$ for an omnidirectional Elfouhaily spectrum with wind speed =10 m/s

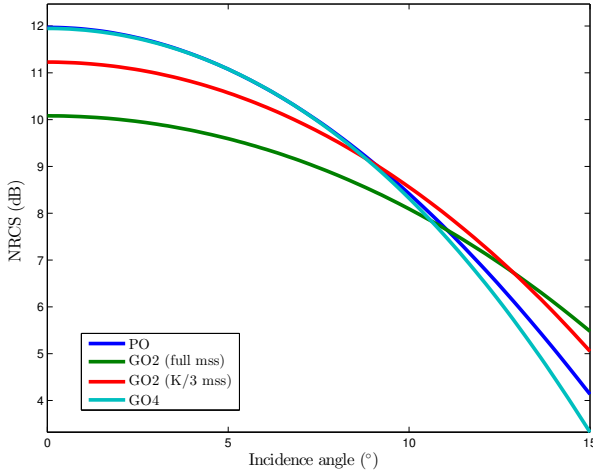


Fig. 4: Comparison of PO, GO2 and GO4 in Ku band with $\alpha = 1.89$ for an omnidirectional Elfouhaily spectrum with wind speed =10 m/s

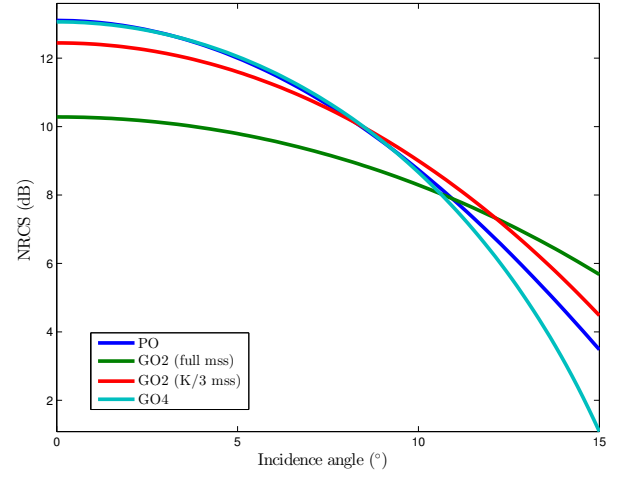


Fig. 5: Comparison of PO, GO2 and GO4 in C band with $\alpha = 2.64$ for an omnidirectional Elfouhaily spectrum with wind speed =10 m/s

IV. ANISOTROPIC CASE

We now develop the GO4 model in the general framework of anisotropic surfaces. Similar calculations have already been derived by one of this author [28] in the high-frequency limit of the PO but the distinction between effective and total msc was not considered. We recall the expression of the directional GO2:

$$\sigma_{GO2}^0(\theta, \varphi) = \frac{|R|^2}{\sqrt{mss_x mss_y}} \sec^4(\theta) \times \exp\left(-\frac{\tan^2 \theta}{2} \left(\frac{\cos^2 \varphi}{mss_x} + \frac{\sin^2 \varphi}{mss_y}\right)\right), \quad (IV.22)$$

with mss_x, mss_y the directional slopes:

$$mss_x = \int k_x^2 \Gamma(\mathbf{k}) d\mathbf{k}, \quad mss_y = \int k_y^2 \Gamma(\mathbf{k}) d\mathbf{k}. \quad (IV.23)$$

The fourth-order Taylor expansion of the structure function is easily found to be:

$$S(x, y) = mss_x x^2 + mss_y y^2 - \frac{1}{12} (msc_x x^4 + 6msc_{xy} x^2 y^2 + msc_y y^4), \quad (IV.24)$$

where msc_x, msc_y, msc_{xy} are the directional curvatures:

$$\begin{aligned} msc_x &= \int k_x^4 \Gamma(\mathbf{k}) d\mathbf{k}, \\ msc_y &= \int k_y^4 \Gamma(\mathbf{k}) d\mathbf{k}, \\ msc_{xy} &= \int k_x^2 k_y^2 \Gamma(\mathbf{k}) d\mathbf{k} \end{aligned} \quad (IV.25)$$

Note that the total mss and msc are given by:

$$\begin{aligned} \text{mss} &= \int k^2 \Gamma(\mathbf{k}) d\mathbf{k} = \text{mss}_x + \text{mss}_y \\ \text{msc} &= \int k^4 \Gamma(\mathbf{k}) d\mathbf{k} = \text{msc}_x + \text{msc}_y + 2\text{msc}_{xy} \end{aligned} \quad (\text{IV.26})$$

Straightforward calculations very similar to those employed in the isotropic case lead to the following formula for the directional GO4 approximation:

$$\begin{aligned} \sigma_{GO4}^0(\theta, \varphi) &= \sigma_{GO2}^0(\theta, \varphi) \left\{ 1 + \frac{1}{96K^2 \cos^2 \theta} \right. \\ &\times \left[\frac{6\text{msc}_{xy}}{\text{mss}_x \text{mss}_y} H_2(X) H_2(Y) \right. \\ &\left. \left. + \frac{\text{msc}_x}{\text{mss}_x^2} H_4(X) + \frac{\text{msc}_y}{\text{mss}_y^2} H_4(Y) \right] \right\} \end{aligned} \quad (\text{IV.27})$$

where the variables X, Y are given by:

$$X = \frac{\tan \theta \cos \varphi}{\sqrt{\text{mss}_x}}, \quad Y = \frac{\tan \theta \sin \varphi}{\sqrt{\text{mss}_y}}, \quad (\text{IV.28})$$

and H_n are the Hermite polynomials:

$$H_n(u) = (-1)^n e^{u^2/2} \frac{d^n}{du^n} e^{-u^2/2}. \quad (\text{IV.29})$$

It is interesting to consider the directional GO4 formula (IV.27) in the particular case of a bi-harmonic spectrum, such as Elfouhaily unified spectrum:

$$\Gamma(k, \varphi) = \frac{1}{2\pi k} \Gamma_0(k) (1 + \Delta(k) \cos(2\varphi)) \quad (\text{IV.30})$$

In addition to the total or isotropic mss and msc, it is then useful to introduce the *anisotropic* mss and msc, referred to by a “i” or “a” subscript:

$$\begin{aligned} \text{mss}_i &= \int k^2 \Gamma_0(k) dk; \quad \text{mss}_a = \int k^2 \Gamma_0(k) \Delta(k) dk \\ \text{msc}_i &= \int k^4 \Gamma_0(k) dk; \quad \text{msc}_a = \int k^4 \Gamma_0(k) \Delta(k) dk \end{aligned} \quad (\text{IV.31})$$

We then have the simple relations:

$$\begin{aligned} \text{mss}_{x/y} &= \frac{1}{2} \left(\text{mss}_i \pm \frac{\text{mss}_a}{2} \right) \\ \text{msc}_{x/y} &= \frac{1}{4} \left(\frac{3}{2} \text{msc}_i \pm \text{msc}_a \right) \\ 6\text{msc}_{xy} &= \text{msc}_x + \text{msc}_y \end{aligned} \quad (\text{IV.32})$$

This reduces the number of slopes and curvature parameters from 5 to 4 and allows it to calculate them through one-dimensional integrals only.

V. NON-GAUSSIAN CORRECTIONS

In the case of a weakly non-Gaussian surface, the Kirchhoff integral admits corrective terms corresponding to the cumulant expansion of the two-point characteristic function:

$$\begin{aligned} \sigma_{PO}^0 &= K^2 \sec^2(\theta) |R|^2 \\ &\times \frac{1}{\pi} \int d\mathbf{r} e^{i\mathbf{Q}_H \cdot \mathbf{r}} e^{-\frac{1}{2} Q_z^2 S(\mathbf{r}) + i\frac{1}{6} Q_z^3 S_3(\mathbf{r}) + \frac{1}{24} Q_z^4 S_4(\mathbf{r})}, \end{aligned} \quad (\text{V.33})$$

where S_3 and S_4 are the skewness and kurtosis function, respectively:

$$\begin{aligned} S_3(\mathbf{r}) &= \langle (\eta(\mathbf{r}) - \eta(0))^3 \rangle \\ S_4(\mathbf{r}) &= \langle (\eta(\mathbf{r}) - \eta(0))^4 \rangle - 3(\langle (\eta(\mathbf{r}) - \eta(0))^2 \rangle)^2 \end{aligned} \quad (\text{V.34})$$

The skewness and kurtosis functions are governed by the skewness and excess kurtosis of slopes for small arguments:

$$\begin{aligned} S_3(x, y) &= \lambda_{30} \text{mss}_x^{3/2} x^3 + \lambda_{03} \text{mss}_y^{3/2} y^3 \\ &+ 3\lambda_{21} \text{mss}_x \text{mss}_y^{1/2} x^2 y + 3\lambda_{12} \text{mss}_y \text{mss}_x^{1/2} x y^2 \\ S_4(x, y) &= \lambda_{40} \text{mss}_x^2 x^4 + \lambda_{04} \text{mss}_y^2 y^4 \\ &+ 6\lambda_{22} \text{mss}_x \text{mss}_y x^2 y^2 \end{aligned} \quad (\text{V.35})$$

where the dimensionless coefficients λ_{mn} are defined by:

$$\lambda_{mn} = \frac{\langle (\partial_x \eta)^m (\partial_y \eta)^n \rangle}{\langle (\partial_x \eta)^2 \rangle^{m/2} \langle (\partial_y \eta)^2 \rangle^{n/2}} \quad (\text{V.36})$$

We do not detail the calculations leading to the GO4 NRCS in the non-Gaussian case, as they are very similar to those employed in the Gaussian case. The Taylor expansions of S_3 and S_4 can be combined with the fourth-order expansion (IV.24) of the structure function and injected in the non-Gaussian expression (V.33) of the PO NRCS. The terms of order 3 and 4 in the exponential are assumed small and linearized out of the exponential. This reduces the Kirchhoff integral to a two-dimensional Fourier Transform of a Gaussian function multiplied by a bi-variate polynomial of fourth degree. In this way we obtain the GO4 formula with skewness and kurtosis correction:

$$\begin{aligned}
\sigma_{GO4}^0 &= \sigma_{GO2}^0 \times \\
&\left\{ 1 + \frac{1}{24Q_z^2} \left[6 \left(\frac{m_{sc_{xy}}}{m_{ss_x} m_{ss_y}} + \lambda_{22} Q_z^2 \right) H_2(X) H_2(Y) \right. \right. \\
&+ \left(\frac{m_{sc_x}}{m_{ss_x}^2} + \lambda_{40} Q_z^2 \right) H_4(X) + \left(\frac{m_{sc_y}}{m_{ss_y}^2} + \lambda_{04} Q_z^2 \right) H_4(Y) \\
&+ \frac{1}{6} \left[3\lambda_{21} H_2(X) H_1(Y) + 3\lambda_{12} H_1(X) H_2(Y) \right. \\
&\left. \left. + \lambda_{30} H_3(X) + \lambda_{03} H_3(Y) \right] \right\}
\end{aligned} \tag{V.37}$$

A resembling formula was proposed in [16] based on a cumulant expansion of the structure function. This last result is, however, different in as much as fourth-order terms in the polynomial expansion stem uniquely from non-vanishing cumulants (that is the very non-Gaussian nature) of the slope distribution and not from the proper geometrical curvature of the surface. An interesting particular case is the isotropic surface for which we have:

$$\begin{aligned}
m_{ss_x} &= m_{ss_y} = \frac{1}{2} m_{ss} \\
m_{sc_x} &= m_{sc_y} = 3m_{sc_{xy}} = \frac{3}{8} m_{sc_e} \\
\lambda_{30} &= \lambda_{03} = \lambda_{12} = \lambda_{21} = 0 \\
\lambda_{40} &= \lambda_{04} = 3\lambda_{22} = \lambda_4
\end{aligned} \tag{V.38}$$

After some calculations we find that the expression (V.37) can be simplified to:

$$\sigma_{GO4}^0 = \sigma_{GO2}^0 \left[1 + \left(\frac{m_{sc_e}}{4Q_z^2 m_{ss}^2} + \frac{\lambda_4}{6} \right) \left(\frac{\tan^4 \theta}{m_{ss}^2} - 4 \frac{\tan^2 \theta}{m_{ss}} + 2 \right) \right] \tag{V.39}$$

Hence we recover the isotropic NRCS of the Gaussian case by augmenting the effective msc with the contribution of the excess kurtosis, that is with obvious notations:

$$m_{sc_e|NG} = m_{sc_e|G} + \frac{2}{3} \lambda_4 m_{ss}^2 Q_z^2 \tag{V.40}$$

Figure 6 shows the respective contributions of the Gaussian msc and its non-Gaussian correction with the value $\lambda_4 = 0.4$ corresponding to the quasi-constant value found by Cox and Munk [29] in their famous experiment (we discard directionality with respect to wind vector). The kurtosis correction becomes important in Ka band and can increase the effective msc by about 50%.

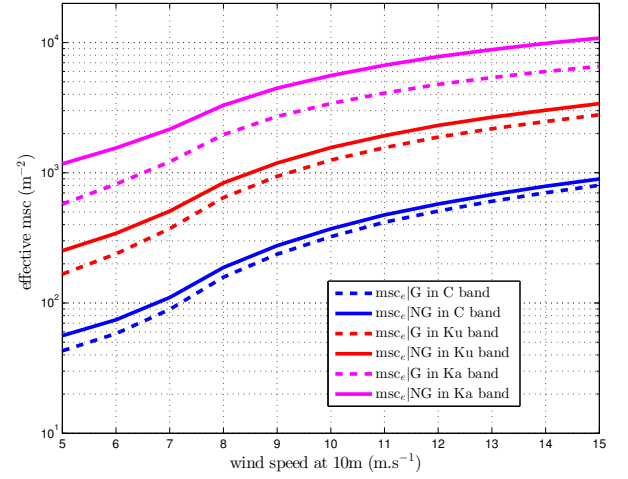


Fig. 6: Gaussian (G) and Non-Gaussian (NG) msc for the omnidirectional Elfouhaily spectrum in different bands.

In the introduction of the kurtosis correction to the effective msc, it is important to keep in mind that the value 0.4 experimentally reported by Cox and Munk is not only due to the peakedness of the slope distribution (very small and very large slopes being more frequent than predicted by the Gaussian distribution) but also on the compound nature of sea slope statistics as was explained in [30]. Hence, fluctuations of statistics across the different sea patches results in an augmentation of the effective msc based on a statistically homogeneous model.

VI. ESTIMATION OF THE MSS AND MSC FROM EXPERIMENTAL DATA

A. Estimation procedure

The main advantage of the two-parameter GO4 model is the possibility to estimate directly the total mss, which is an intrinsic parameter of the sea surface, and not the “mss seen by the radar” which depends on the EM wavelength. In addition, it provides an accurate parametrization of the backscattering cross-section in a wide angular domain around nadir with the additional knowledge of the effective msc.

For this illustration of the GO4 concept, we will restrict the consideration to the omnidirectional NRCS, a more detailed study being left for further work. We recall that this quantity is obtained by averaging all possible azimuthal direction φ at the same incidence angle θ :

$$\sigma_{omni}^0(\theta) = \frac{1}{2\pi} \int_0^{2\pi} d\varphi \sigma^0(\theta, \varphi) \tag{VI.41}$$

The omnidirectional NRCS will be treated with a isotropic GO4 model, even though this introduce small bias in the estimation of the mss and msc (see the discussion further).

Our analysis will be based on several near-nadir data sets from the literature. Since the different data sets are well-documented we will not enter in their description and simply refer to the main publications. We will use the Ka-band airborne scanning radar altimeter (SRA) data of the Southern Ocean Waves Experiment (SOWEX, [31], [32]), the Ku/C Jason2 altimeter data, data from the Ku band precipitation radar from the Tropical Rainfall Measuring Mission [33], [34] and the Ka-band airborne scatterometer data described in [35].

The difficulty in evaluating the mss and msc parameters from spaceborne or airborne data is the uncertainty linked to the data calibration. However, whenever a certain range of incidence angle is available, the joint estimation of mss and msc can be performed on the basis of relative values (i.e. non calibrated) of the NRCS. In that case, the parameter estimation is obtained upon minimization of the following cost function in a certain range of incidence:

$$\Phi = \sum_{\theta < \theta_{max}} |\sigma_{data}^0(\theta) - \sigma_{GO4}^0(mss, msc, \theta)|^2, \quad (VI.42)$$

where the NRCS are taken in dB and normalized by their value at nadir. This has been done for the SRA data in Ka band and the TRMM data in Ku band for which ranges of incidence of 0 – 25 degrees and 0 – 18 degrees, respectively, are available. It is important to note that the accuracy of the parameter estimation is slightly dependent on the chosen range of incidence. It should be chosen as large as possible in order to better separate the quartic behavior (GO4) from the quadratic behavior (GO2) with respect to the variable $\tan \theta$ but, on the other hand, should respect the validity domain of the GO4 approximation. This sensibility of the estimated shape parameters to the incidence span has been known for a long time in the case of the estimation of the single radar-mss from a GO2 model (this is discussed in detail in [36]). It requires some a priori knowledge of the incidence span over which the model is expected to hold. From the systematic analysis of section III with synthetic data at various wind speeds (exemplified on Figures 3, 4 and 5) we have seen that this validity domain increases with both EM frequency and wind speed. For altimeter data where only the nadir NRCS is available we will rely on its absolute level. The effective msc is then evaluated from Cox and Munk mss [29], which we abbreviate to “CM-mss”. This has been done with Jason2 data in C and Ku band as well as the Ka band airborne measurements from [35].

B. TRMM

Figure 7 shows the total mss inverted from the omnidirectional TRMM NRCS using either the simple GO2 model or the joint inversion of mss and msc with the GO4 model. A comparison is given with the total CM-mss and the radar-filtered mss calculated with Elfouhaily spectral model using the usual frequency cut-off at $K/3$. As seen, the mss obtained from the mere GO2 model is close to the radar-filtered mss while the mss estimated from GO4 is in excellent agreement with the total mss. The effective msc estimated with GO4 is shown on Figure 8 and is found in excellent agreement with the effective msc derived from the analytical spectra (in particular Bringer and Kudryavstev models). In the calculation of the effective msc we have used formula (II.18) together with the non-Gaussian correction (V.40).

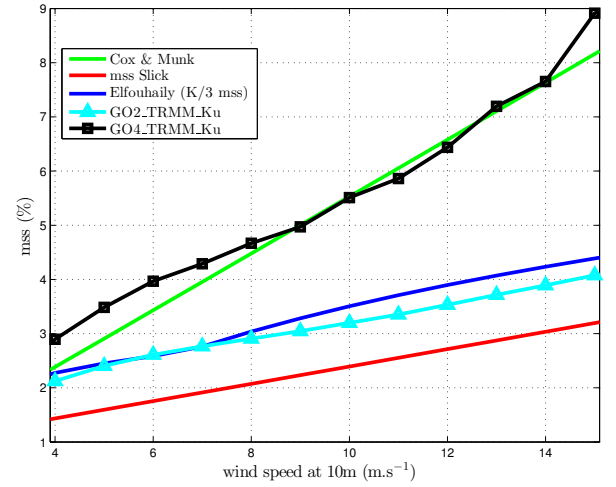


Fig. 7: Estimation of the mss with the GO2 and GO4 model for the TRMM Ku data. A comparison is given with the filtered mss for different spectra.

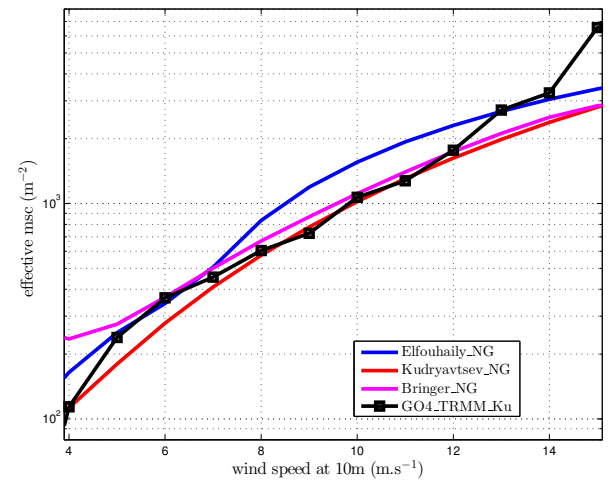


Fig. 8: Same as Figure 7 for the msc

The knowledge of the total mss and effective msc makes it possible to obtain the absolute level of NRCS

at nadir. From equation II.20 we have:

$$\sigma^0(0) = \frac{|R|^2}{mss} \left(1 + \frac{mss_e}{8K^2 mss^2} \right) \quad (\text{VI.43})$$

Figure 9 shows the recalibration of the relative TRMM data at nadir and a comparison with the absolute values. A discrepancy from 0.5 (small winds) to 1 dB (larger winds) is observed, suggesting that the absolute values of the TRMM data might be slightly underestimated.

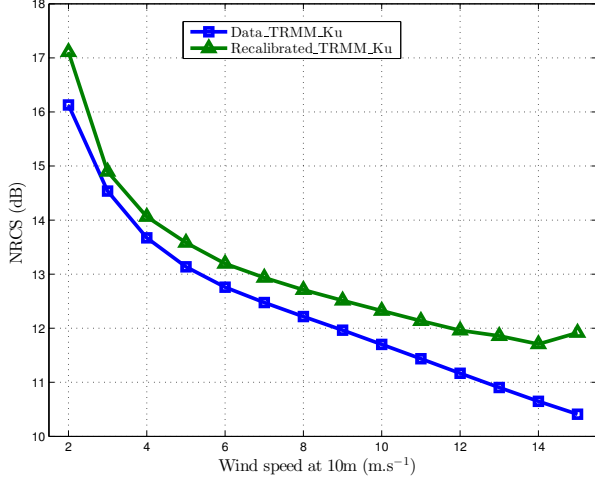


Fig. 9: Recalibration of TRMM relative data and comparison with the absolute values

C. SRA

The sea state conditions encountered during the SOWEX experiment (South West Tasman Sea) were found close to infinite fetch [31], [32], which makes the comparison with other satellite data and CM-mss meaningful. The relative values (i.e normalized by their maximum) of the omnidirectional NRCS recorded by the SRA were fitted in the form ([32]):

$$\ln(\sigma_{rel}^0)(\theta) = -AS^2 + BS^4, \quad (\text{VI.44})$$

with $S = \tan \theta$ and $B = 0.567A^{1.332}$. The value of A are not given in the publication but have been provided by one of the authors (B. Chapron). The wind speed dependence between 3 and 16 m/s is as follows: $A(3)=2.36, A(4)=46.73, A(5)=42.55, A(6)=39.37, A(7)=37.18, A(8)=34.36, A(9)=29.67, A(10)=27.17, A(11)=25.00, A(12)=23.30, A(13)=21.80, A(14)=20.48, A(15)=19.31, A(16)=18.27$. Figure 10 shows the estimation of the mss after the isotropic GO2 and GO4 models, respectively. As expected, the estimated mss with GO4 is consistent with CM-mss while the mss parameter inferred from GO2 is consistent with a radar mss in Ka band (calculated here with help of Elfouhaily spectral model). Note, however,

that the GO4-mss is found 10 – 20% smaller than CM-mss at moderate wind speeds. Possible explanations for this reduced slope can be hypothesized. A first artifact is the discarding of directional effects when estimating the total mss with an isotropic model. Denoting $\beta = mss_y/mss_x$ the ratio of upwind to crosswind mss, it was shown in [30] that the mss estimated from the shape parameter of the GO2 model is in fact lowered by a factor $4\beta/(1+\beta)^2$ with respect to the actual mss. For anisotropic wind-wave sea states such as those encountered in Cox and Munk experiment ($\beta \simeq 0.65$) the reduction factor is negligible (0.95). However, for more pronounced anisotropy due to young sea states or the presence of a swell aligned with wind, a stronger discrepancy can be achieved. Another source of difference with CM-mss is the presence of swell which is believed to decrease the spectral density in the short-wave portion of intermediate-scale waves [25], [37]. This is consistent with the low mss observed at intermediate wind speeds (6-10 m/s) for which run days a strong swell was reported [31].

Figure 11 shows the estimation of the non-Gaussian effective msc from the GO4 model and a comparison with the value predicted by the different spectra under a peakedness correction of $\lambda_4 = 0.4$. A good agreement is reached at moderate and large wind speed while the estimated msc is significantly lower than its predicted values at small wind speed. Again, we hypothesize that this discrepancy is due, at least partially, to the influence of swell on the short-wave spectrum.

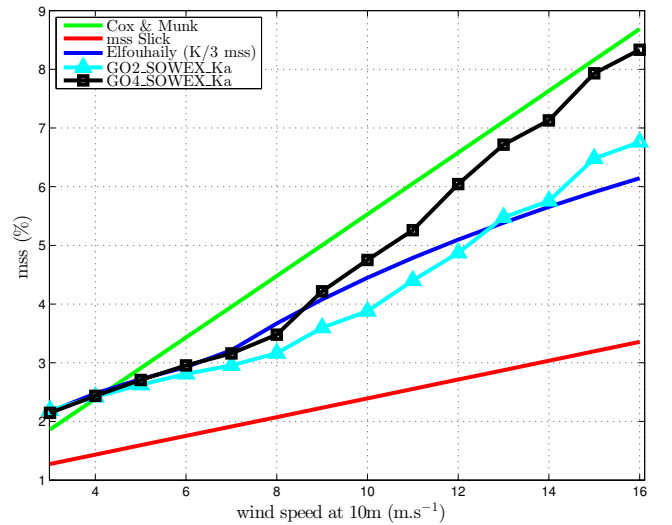


Fig. 10: mss versus wind speed from SOWEX Ka data.

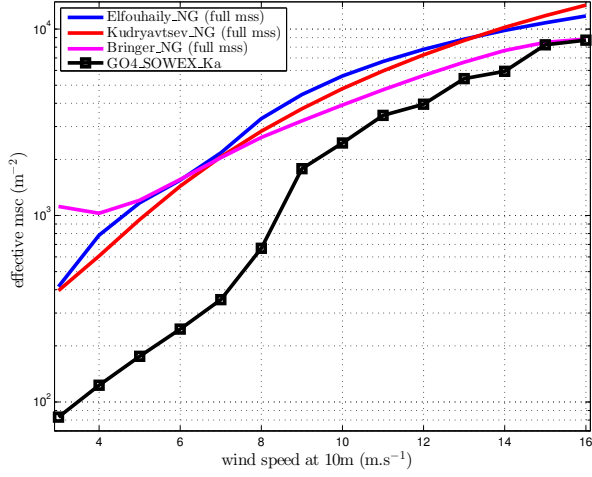


Fig. 11: msce versus wind speed from SOWEX Ka data.

D. Jason2

The absolute nadir NRCS of Jason 2 in C and Ku band have been used to estimate the effective msc assuming the mss is given by Cox and Munk measurements. Figure 12 shows the mss inverted from GO2 at nadir in Ku and C band and a comparison with the optical mss from Cox and Munk and the radar mss according to different spectral models. As expected, the GO2-inverted mss is consistent with a filtered mss and much smaller than the total mss: it is found equal to about 50-60 % of the optical mss in Ku band (consistently with the findings of [38]) and 35-45 % in C band. The effective msc is in good agreement with the theoretical predictions according to the different spectral models.

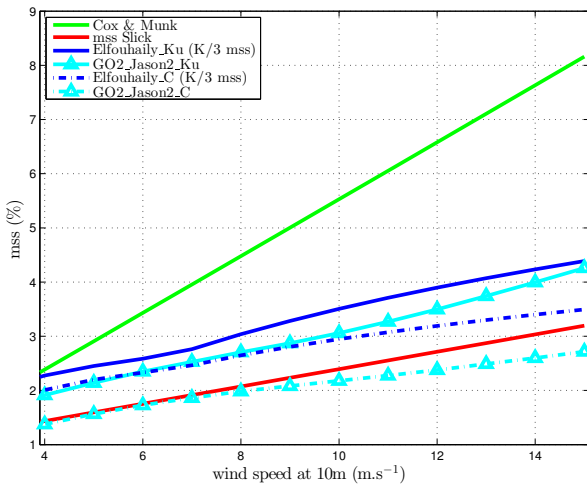


Fig. 12: mss versus wind speed from Jason2 C and Ku data.

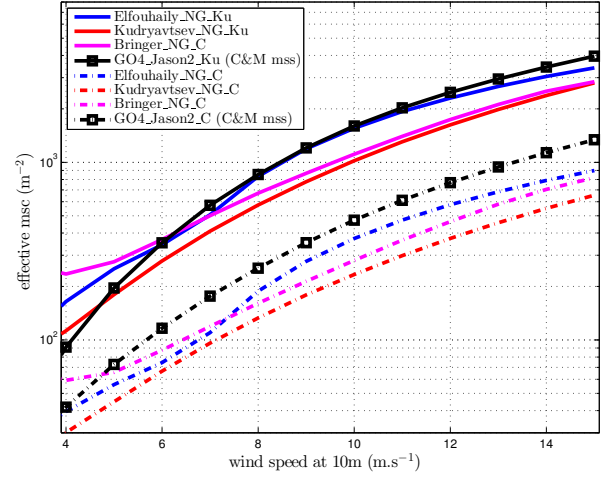


Fig. 13: msce versus wind speed from Jason2 C and Ku data.

E. Cox and Munk, slick case

There are no available near-nadir L band data to test the GO4 model. However, an approximate derivation of the L band msc can be inferred from Cox and Munk sea surface slopes measurements. In their experiment, these authors also measured the “slick” mss corresponding to the case of oil slickened surface. It is estimated that the viscous effect of surfactant damps the short-scale component smaller than about 30-40 cm at the sea surface. Hence, the slick mss can be seen as a radar-filtered mss at a cut-off corresponding to the L band wave number. Assuming the GO2 model with filtered mss to be close to the actual NRCS at nadir we have the following relationship with the effective L band msc which can thus be inverted:

$$\frac{|R|^2}{mss_{slick}} = \frac{|R|^2}{mss_{clean}} \left(1 + \frac{mss_e}{8K^2 mss_{clean}^2} \right) \quad (VI.45)$$

The L band effective msc can be extracted easily from this relation.

F. Vandemark et al.

The airborne experiment described in [35] provides additional nadir Ka band measurements of the NRCS in ocean conditions. We have used the absolute values of the NRCS reported in this work assuming the total mss is consistent with Cox and Munk observations to obtain the Ka band effective msc. The estimation was not conclusive at small wind speeds where negative values of the msc occurred. This might be due either to a discrepancy with CM conditions or to a bias in the absolute NRCS.

Figures 14 and 15 summarize our findings on the basis of available experimental data sets. They show,

respectively, the evolution of the effective msc as a function of wind speed for the different radar bands and a function of the frequency band at different wind speeds. The effective msc is augmented by several order of magnitudes from L to Ka band and by one order of magnitude from small to large wind speeds. The cross-over observed between Ku and Ka-band at small wind speed is probably due to the peculiar sea state of the SOWEX experiment and the corresponding low msc as discussed above.

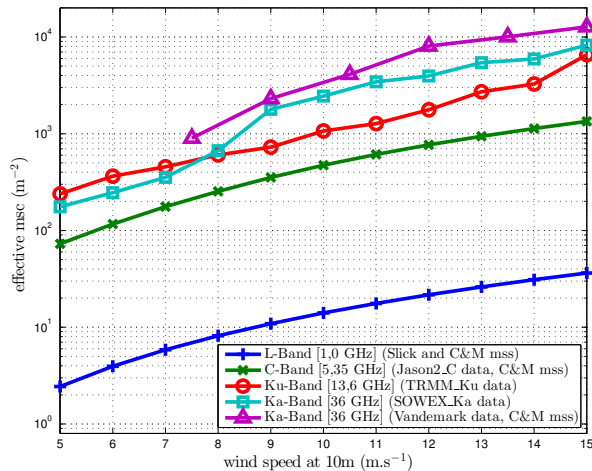


Fig. 14: Effective msc versus wind speed for the different frequency bands

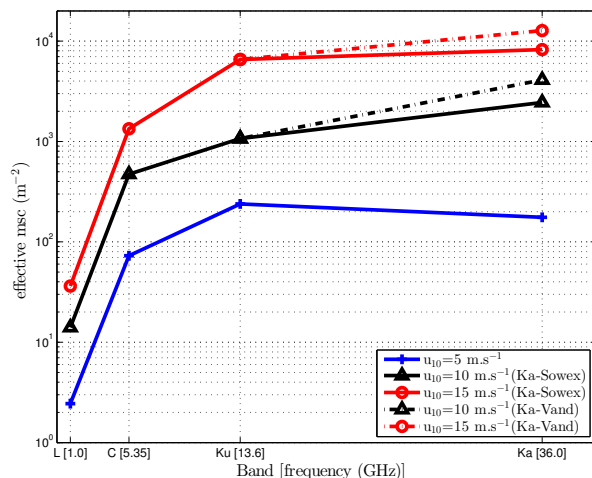


Fig. 15: Effective msc versus radar frequency at different wind speeds

VII. CONCLUSIONS

The GO4 is a simple scattering model with a reduced number of parameters (2 in the isotropic case, 5 in the directional case) which enjoys the same accuracy as the PO model in a wide range of incidence away from nadir. It avoids the heuristic choice of a “radar-mss” or filtered mss used in the classical GO2 model, which is

replaced by the total mss and a diffraction correction quantified by an effective msc depending on the EM frequency. While the total mss is an ill-defined quantity as it is dramatically sensitive to scales much smaller than the radar wavelength and questions the microscopic nature of the sea surface, the effective msc involves only scales comparable to the radar wavelength and quantifies the diffraction process at the given wavelength. On the contrary, the total mss is a well-defined quantity as the decrease of the surface spectrum ensures convergence of its second moment. We have provided a way to calculate the effective msc from the knowledge of the surface spectrum and given estimations based on some classical spectral models as well as experimental data. Beside an accurate and simple parameterization of the scattering cross-section at moderate incidence, the GO4 is found useful in estimating the total mss (and not the radar-mss) as well as recalibrating relative data. Another interesting feature of the GO4 approach is the capability to absorb non-Gaussian effects (due to the peakedness of wave slopes and compound wave statistics) in the same analytical framework at the simple cost of an augmented msc. At this stage, the estimation process has been limited to omnidirectional quantities, the full study of the directional case being left for further work.

ACKNOWLEDGMENTS

Olivier Boisot PhD is granted by CNES and CLS. Frédéric Nougier acknowledges support of the CNRS and the University of Toulon (chaire mixte).

REFERENCES

- [1] G.R. Valenzuela. Theories for the interaction of electromagnetic and oceanic waves- a review. *Boundary-Layer Meteorology*, 13(1):61–85, 1978.
- [2] T. Elfouhaily and C.A. Guérin. A critical survey of approximate scattering wave theories from random rough surfaces. *Waves in Random and Complex Media*, 14(4):1–40, 2004.
- [3] A. Voronovich. Small-slope approximation for electromagnetic wave scattering at a rough interface of two dielectric half-spaces. *Waves in Random and Complex Media*, 4(3):337–367, 1994.
- [4] A. G. Voronovich. *Wave scattering from rough surfaces*. Springer Series on Wave Phenomena. Springer, 1994.
- [5] AG Voronovich and VU Zavorotny. Theoretical model for scattering of radar signals in k u-and c-bands from a rough sea surface with breaking waves. *Waves in Random Media*, 11(3):247–269, 2001.
- [6] AA Mouche. A simplified asymptotic theory for ocean surface electromagnetic wave scattering. *Waves in Random and Complex Media*, 17(3):321–341, 2007.
- [7] G. Soriano and C.A. Guérin. A cutoff invariant two-scale model in electromagnetic scattering from sea surfaces. *Geoscience and Remote Sensing Letters, IEEE*, 5(2):199–203, 2008.
- [8] C.A. Guérin, G. Soriano, and B. Chapron. The weighted curvature approximation in scattering from sea surfaces. *Waves in Random and Complex Media*, 14(3):349–363, 2010.

- [9] PJ Lynch. Curvature corrections to rough-surface scattering at high frequencies. *The Journal of the Acoustical Society of America*, 47(3B):804–815, 1970.
- [10] Ernesto Rodriguez. Beyond the kirchhoff approximation. *Radio Science*, 24(5):681–693, 1989.
- [11] Ernesto Rodríguez. Beyond the kirchhoff approximation ii electromagnetic scattering. *Radio science*, 26(1):121–132, 1991.
- [12] DR Thompson, TM Elfouhaily, and JL Garrison. An improved geometrical optics model for bistatic GPS scattering from the ocean surface. *IEEE Transactions on Geoscience and Remote Sensing*, 43(12):2810–2821, 2005.
- [13] D Hauser, G Caudal, Sebastien Guimbard, and AA Mouche. A study of the slope probability density function of the ocean waves from radar observations. *Journal of Geophysical Research: Oceans* (1978–2012), 113(C2), 2008.
- [14] AA Mouche, B. Chapron, N. Reul, D. Hauser, and Y. Quilfen. Importance of the sea surface curvature to interpret the normalized radar cross section (DOI 10.1029/2006JC004010). *J. Geophys. Res.*, 112(C10):10002, 2007.
- [15] Ninoslav Majurec, Joel T Johnson, Simone Tanelli, and Stephen L Durden. Comparison of model predictions with measurements of ku-and ka-band near-nadir normalized radar cross sections of the sea surface from the genesis and rapid intensification processes experiment. *IEEE Trans. Geosci. and Remote Sens.*, 52(9):5320 – 5332, 2014.
- [16] Suzanne T McDaniel. Microwave backscatter from non-gaussian seas. *Geoscience and Remote Sensing, IEEE Transactions on*, 41(1):52–58, 2003.
- [17] I.M. Fuks. Backscattering from a statistically rough 2-d surface: Diffraction corrections to geometrical optics cross sections. *Radio Science*, 42(6):RS6S25, 2007.
- [18] I. Fuks. Diffraction corrections to go backscattering from a perfectly conducting 3-d rough surface. *Radio Sci*, 43, 2008.
- [19] Sébastien Guimbard. *Interprétation et modélisation de mesures à distance de la surface marine dans le domaine micro-onde*. PhD thesis, Versailles-St Quentin en Yvelines, 2010.
- [20] Alexandra Bringer, Charles-Antoine Guérin, Bertrand Chapron, and Alexis Mouche. Peakedness effects in near-nadir radar observations of the sea surface. *Geoscience and Remote Sensing, IEEE Transactions on*, 50(9):3293–3301, 2012.
- [21] T. Elfouhaily, B. Chapron, K. Katsaros, and D. Vandemark. A unified directional spectrum for long and short wind-driven waves. *J. Geophys. Res.*, 102(C7):15781–15796, July 1997.
- [22] Alexandra Bringer, Bertrand Chapron, Alexis Mouche, and Charles-Antoine Guérin. Revisiting the short-wave spectrum of the sea surface in the light of the weighted curvature approximation. *IEEE Trans. Geosci. and Remote Sens.*, 52(1):679–689, 2014.
- [23] V. Kudryavtsev, D. Hauser, G. Caudal, and B. Chapron. A semiempirical model of the normalized radar cross-section of the sea surface 1. background model. *J. Geophys. Res.*, 108(C3):8054, 2003.
- [24] V. Kudryavtsev, D. Hauser, G. Caudal, and B. Chapron. A semiempirical model of the normalized radar cross-section of the sea surface: 2. Radar modulation transfer function. *J. Geophys. Res.*, 108(C3):8055, 2003.
- [25] Paul A Hwang. Observations of swell influence on ocean surface roughness. *Journal of Geophysical Research: Oceans* (1978–2012), 113(C12), 2008.
- [26] MV Yurovskaya, VA Dulov, Bertrand Chapron, and VN Kudryavtsev. Directional short wind wave spectra derived from the sea surface photography. *Journal of Geophysical Research: Oceans*, 118(9):4380–4394, 2013.
- [27] Gary S Brown. Backscattering from a gaussian-distributed perfectly conducting rough surface. *Antennas and Propagation, IEEE Transactions on*, 26(3):472–482, 1978.
- [28] Frédéric Nouguier. *Diffraction électromagnétique par la surface océanique: influence des nonlinéarités et de lécume*. PhD thesis, Aix-Marseille Université, 2009.
- [29] C. Cox and W. Munk. Statistics from the sea surface derived from the sun glitter. *J. Marine Res.*, 13:198–227, 1954.
- [30] B. Chapron, V. Kerbaol, D. Vandemark, and T. Elfouhaily. Importance of peakedness in sea surface slope measurements and applications. *Journal of geophysical research*, 105:17, 2000.
- [31] Michael L Banner, Wei Chen, Edward J Walsh, Jorgen B Jensen, Sunhee Lee, and Chris Fandry. The southern ocean waves experiment. part i: Overview and mean results. *Journal of physical oceanography*, 29(9):2130–2145, 1999.
- [32] E.J. Walsh, M.J. Banner, C.M. Wrieth, D.C. Vandemark, B. Chapron, J. Jensen, and L. See. The Southern Ocean Waves Experiment. Part III: Sea Surface Slope Statistics and Near-Nadir Remote Sensing. *Journal of Physical Oceanography*, 38:670–684, 2008.
- [33] C. Kummerow, W. Barnes, T. Kozu, J. Shiue, and J. Simpson. The tropical rainfall measuring mission (trmm) sensor package. *Journal of Atmospheric and Oceanic Technology*, 15(3):809–817, 1998.
- [34] N. Tran, B. Chapron, and D. Vandemark. Effect of long waves on ku-band ocean radar backscatter at low incidence angles using trmm and altimeter data. *Geoscience and Remote Sensing Letters, IEEE*, 4(4):542–546, 2007.
- [35] D. Vandemark, B. Chapron, J. Sun, G.H. Crescenti, and H.C. Graber. Ocean wave slope observations using radar backscatter and laser altimeters. *J. Phys. Oceanogr.*, 34:2825–2842, december 2004.
- [36] E.J. Walsh, D.C. Vandemark, C.A. Friehe, S.P. Burns, and D. Khelif. Measuring sea surface mean square slope with a 36 GH scanning radar altimeter. *J. Geophys. Res.*, 183(C6):12613–12602, 1998.
- [37] Paul A Hwang and William J Plant. An analysis of the effects of swell and surface roughness spectra on microwave backscatter from the ocean. *Journal of Geophysical Research: Oceans* (1978–2012), 115(C4), 2010.
- [38] FC Jackson, WT Walton, DE Hines, BA Walter, and CY Peng. Sea surface mean square slope from ku-band backscatter data. *Journal of Geophysical Research*, 97(C7):11411–11, 1992.